CLM-P647

UKAEA

Preprint

SPECIES AND IMPURITY MEASUREMENTS IN INTENSE NEUTRAL BEAMS ON DITE TOKAMAK

S. J. FIELDING
D. STORK

CULHAM LABORATORY
Abingdon Oxfordshire

1981

CLM-P647

SPECIES AND IMPURITY MEASUREMENTS IN INTENSE NEUTRAL BEAMS ON DITE TOKAMAK

S.J. Fielding and D. Stork*

Culham Laboratory, Abingdon, Oxon., OX14 3DB, UK
(Euratom/UKAEA Fusion Association)

*JET Joint Undertaking, Abingdon, Oxon., OX14 3DB, UK

ABSTRACT

Species and impurity measurements have been made on the DITE Phase II neutral injection beams using both optical and charge exchange techniques. The species measurements from the two techniques are in good agreement with one another.

Hydrogen-bearing impurities originating from the sources have been detected and quantitative estimates of impurity content have been made. The principal impurity ions generated from the sources are identified as H_3O^+ and CH_5^+ at the few per cent level. Measurements have also been made of spectral line emission from C^{3+} and O^{6+} in DITE plasmas with and without neutral injection in operation. Doppler shifted spectra are observed and their origin is discussed.

June 1981

(Submitted for publication in Nuclear Fusion)

1. INTRODUCTION

High power (1MW) neutral injection is used in the DITE tokamak as a means of achieving high ion temperatures and high plasma pressure [1, 2]. A detailed knowledge of the hydrogen energy spectrum of the beams is important in order to interpret experimental results. The energy spectrum is related to the species yield of the ion sources producing the beams, and the ratios of the yields of the various hydrogen species are important parameters in source performance. We report here the results of in situ beam energy measurements by spectroscopy and neutral particle energy analysis.

Associated with the injection pulse into DITE there is invariably a large increase in radiation from the plasma, resulting from enhanced impurity line emission. There are three possible explanations for this: (1) impurities in the neutral beam, (2) enhanced sputtering or desorption of impurities from the torus walls/limiters, (3) beam excitation of impurities already in the plasma. Impurities entering the plasma with the neutral beam are particularly harmful since they are deposited deep into the plasma where they can be confined for long times. For 1MW of injection into a medium density plasma in DITE ($\bar{n}_e$ = 2.10^{19} m^{-3}) a 5% impurity contamination of the beam particle flux would result in an impurity density in the plasma of $\sim$ 2.5%. In this paper we describe measurements made to determine the impurity content of the DITE neutral injection beams.

A plan view of DITE is shown in Figure 1, with the relevant diagnostics marked. The injectors and beam lines have been described elsewhere [3,4]. In brief, each beam line is 3.6m long and is fitted with two 25keV, 30A magnetic multipole ion sources. Ions from the source are neutralised in a 1m gas neutraliser box in front of each

source. The plasma sources are operated in hydrogen at filling pressures between 3 and 30 x 10^{-3}torr. Each beam line is pumped by a large volume liquid helium cryopump (hydrogen pumping speed 150,000 litres/sec) and the background pressure between pulses is $\sim 10^{-7}$ torr. Beams of 50-100ms duration are extracted from the sources. Any residual ions in the beam leaving the neutraliser can be dumped onto a cooled copper beam-dump using magnetic deflector coils placed in the vacuum underneath the cryopump.

2. SPECIES MEASUREMENTS

2.1 Optical measurements

The extracted beams from the A line sources were viewed directly, along a line of sight tangential to the torus, by a 0.5m Czerny-Turner spectrometer [5] equipped with an internal vibrating mirror for taking fast wavelength scans (Fig 1). The instrument was centred at H_α (656.3nm) and had a linear response in a ± 6nm range about this line. This range could be scanned by the spectrometer in about 2ms. The observed H_α spectra showed both Doppler shifted and unshifted components during beam extraction. These arose from the following reactions:

$$H_f^o + H_2 \rightarrow H_f^* + H_2 \quad \ldots (1)$$

$$H_f^+ + H_2 \rightarrow H_f^* + H^+ + H \quad \ldots (2)$$

$$H_f^o + H_2 \rightarrow H_f^o + H^* + H \quad \ldots (3)$$

$$H_f^+ + H_2 \rightarrow H_f^+ + H^* + H \quad \ldots (4)$$

where f denotes a fast particle and * the excited state 3s, 3p or 3d.

Reactions (1) and (2) give rise to the Doppler shifted H_α lines whilst (3) and (4) yield unshifted lines. Deuterium gas can be substituted as the target in (1) to (4), yielding shifted H_α and unshifted D_α spectra.

The Doppler shifted spectra can be related directly to the energy spectrum of hydrogen ions and neutrals in the beam. The spectra were studied for beams with and without D_2 gas in the torus and for beams with and without the deflection magnets in use. The effect of reduced pressure in the beam line, achieved by filling the cryopumps with liquid helium, was also recorded.

2.2 Neutral particle analyser measurements

The C line beams were energy analysed using a tangentially-viewing neutral particle analyser (NPA) [6]. Beams were injected into a torus filled with D_2 gas and with a toroidal field of 1.4T. Ions formed in the reaction

$$H_f^o + D_2 \rightarrow H_f^+ + e \ldots\ldots \qquad \ldots (5)$$

were trapped by the toroidal field and circulated until they escaped by the charge-exchange reaction

$$H_f^+ + D_2 \rightarrow H_f^o \ldots\ldots \qquad \ldots (6)$$

Neutrals from reaction (6) were detected by the tangential NPA. An energy spectrum was built up in several shots, the count rate being integrated over a 20ms period during each shot.

3. IMPURITY MEASUREMENTS

Metallic impurities (Cu, W, Mo), due to sputtering and evaporation of electrode and filament material in the sources, have been looked for by a carbon collector probe placed at the end of the beam line [7]. The probe was subsequently analysed by Auger spectroscopy and Rutherford back-scattering techniques. No metals were actually detected and the

sensitivity of the apparatus set an upper limit of one part in 10^4 on the metal impurity content (at mass = 96, nuclear charge = 42).

Light impurities in the beam can result from gas contamination or desorption of impurities (eg water vapour) from the walls and electrodes of the sources. Gas contamination was ruled out by analysis of the source input gas by a mass spectrometer. Desorbed impurities forming hydrogen bearing molecules in the arcs were detected from an analysis of the Doppler-shifted H_α spectra using the vibrating mirror spectrometer. Such impurities undergo acceleration and dissociation to give energetic hydrogen neutrals which can be excited to emit H_α.

Energetic impurities injected into the plasma with the beam can give rise to Doppler-shifted impurity emission from the plasma. This was investigated using a one-metre normal incidence vacuum ultra-violet (NIVUV) spectrometer [8] viewing tangentially into the torus. The NIVUV was used to measure line profiles of carbon and oxygen emission. Wavelength scans were performed on a shot to shot basis over a spectral range of 1nm, with a resolution of 0.05nm. Only two lines had sufficient intensity for detailed Doppler-shift measurements, the C^{3+} doublet ($2s\ ^2S_{\frac{1}{2}} - 2p^2P_{3/2,\frac{1}{2}}$) at 154.8nm and the O^{6+} line ($2s\ ^3S - 2p\ ^3P_2$) at 162.3nm.

4. RESULTS AND DISCUSSION

4.1 Optical spectra

A typical Doppler-shifted spectrum from one of the A line sources is shown in Figure 2(a), for D_2 in the torus, deflectors on and cryo-pumps cooled to liquid helium temperature. The unshifted H_α and D_α lines can be seen, together with Doppler-shifted H_α lines from hydrogen neutrals travelling with velocities corresponding to E_b (the full beam

energy), $E_b/2$, $E_b/3$ and E_b/k where $17 \lesssim k \lesssim 19$.

The components E_b, $E_b/2$ and $E_b/3$ are characteristic of hydrogenic species extracted from low pressure hydrogen plasma sources. The beam leaving the source contains H^+, H_2^+ and H_3^+ ions and the latter two species undergo neutralisation and breakup reactions in the neutraliser to yield particles with energies $E_b/2$ and $E_b/3$. The peak around $E_b/19$ originates from hydrogenic impurity molecules, ionised in the source and then extracted. These undergo neutralisation and breakup reactions yielding low energy hydrogen atoms. For an energy $\sim E_b/19$ an impurity ion with mass $\simeq$ 19amu is required, corresponding probably to OH^+, H_2O^+, H_3O^+ or CH_5^+.

The observed light signals originated from interaction of the beam with D_2 in the torus and H_2 in the beam line, corresponding to reactions (1) to (4). The neutral/ion ratio changes as the beam passes through the neutraliser and the background gas, and it is not possible to derive energy spectra and species ratios directly from a single set of data. However, these can be calculated by taking data both with and without gas in the torus. Defining

$S_D^G(E) \equiv$ signal obtained at energy E with gas in the torus, deflectors on

$S_D^{NG}(E) \equiv$ signal obtained at energy E with no gas, deflectors on,

the quantity $S_D^G(E) - S_D^{NG}(E) = \Delta S(E)$ corresponds to the signal produced by fast neutrals incident on the torus deuterium gas (reaction 1). A small ionic contamination still exists due to reionisation of the beam particles in the torus gas (pressure $\sim 3.10^{-4}$ torr) but this does not substantially affect the results.

The hydrogen energy spectrum of the beam entering the torus, $j_H^o(E)$,

may be obtained from the measured $\Delta S(E)$ values by using the cross-sections for reaction (1), which have been measured between 10 and 35keV beam energy [9]. It may be shown [10] that the number of H_α photons emitted from excited states formed in reaction (1) at beam energy E_b/k ($k = 1,2,3$ etc) in a path length ℓ is given by

$$J_\alpha(E_b/k) = n(E_b/k)\, A\ell N v \sum_\psi \sigma^o_\psi(E_b/k)\, \tau_\psi A_{\alpha\psi} \left[1 - \frac{v\tau_\psi}{\ell}\left(1 - e^{-\ell/v\tau_\psi}\right)\right] \ldots \quad (7)$$

where $\psi \equiv$ 3s, 3p, 3d states

$\sigma^o_\psi(E_b/k) \equiv$ cross section for beam excitation of state ψ at beam energy E_b/k

$\tau_\psi \equiv$ lifetime of excited state ψ

$A_{\alpha\psi} \equiv$ radiative transition probability for H_α decay of state ψ

$v \equiv$ velocity of beam particles at E_b/k

$N \equiv$ neutral gas density

$A \equiv$ beam cross sectional area

$n(E_b/k) \equiv$ density of beam particles at E_b/k

Since the flux of particles $j = nv$, equation (7) can be rearranged to give $j^o_H(E_b/k)$ and hence the ratios of the energy components of the beam entering the torus, relative to the main component

$$\frac{j^o_H(E_b/k)}{j^o_H(E_b)} = \frac{J_\alpha(E_b/k)}{J_\alpha(E_b)} \cdot \frac{\sum_\psi \sigma^o_\psi(E_b)\tau_\psi A_{\alpha\psi}\left[1 - \frac{v(E_b)\tau_\psi}{\ell}\left(1 - e^{-\ell/v(E_b)\tau_\psi}\right)\right]}{\sum_\psi \sigma^o_\psi(E_b/k)\tau_\psi A_{\alpha\psi}\left[1 - \frac{v(E_b/k)\tau_\psi}{\ell}\left(1 - e^{-\ell/v(E_b/k)\tau_\psi}\right)\right]} \ldots \quad (8)$$

Equation (8) can be greatly simplified in the case under consideration. The observation pathlength is relatively long (1.8m) and the lifetimes of the 3s, 3p and 3d states are 160ns, 5.4ns and 15.6ns respectively.

Thus in all cases the exponential terms in (8) are negligible for the three main components of the beam and the quantity $v(E_b)\tau_\psi/\ell \ll 1$ for the 3p and 3d states. Since the J_α's are proportional to the measured ΔS values, with an energy-independent proportionality constant, equation (8) reduces to

$$\frac{j_H^o(E_b/k)}{j_H^o(E_b)} = \frac{\Delta S(E_b/k)}{\Delta S(E_b)} \cdot \frac{\sum_\psi \sigma_\psi^o(E_b)\tau_\psi A_{\alpha\psi} K_\psi(E_b)}{\sum_\psi \sigma_\psi^o(E_b/k)\tau_\psi A_{\alpha\psi} K_\psi(E_b/k)} \qquad \ldots (9)$$

where $$K_\psi = \left[1 - \frac{v(E)}{\ell}\tau_\psi\left(1 - e^{-\ell/v(E)\tau_\psi}\right)\right] \sim 1$$

The values of $A_{\alpha\psi}$ and K_ψ are given in Table I.

A typical result for the hydrogen energy spectrum (ignoring impurities), obtained at source filling pressure $1.5.10^{-2}$ torr and ion current density (j^+) of 190mA/cm^2, is shown in Table II.

It can be shown that the main ion species ratios leaving the source may be written as

$$\frac{j_k^+}{j_1^+} = \frac{j_H^o(E_b/k)}{j_H^o(E_b)} \cdot \frac{1}{k'} \cdot \frac{f^o(E_b)}{f^o(E_b/k)} \qquad \ldots (10)$$

where $f^o(E_b) \equiv$ fraction of the source ions neutralised in the beamline before the deflectors

$j_k^+ \equiv$ ion current of mass k amu leaving the source

$k' \equiv$ number of hydrogen nuclei yielded on breakup of original ion.

$f^o(E)$ is known from measurements on a test rig and hence the species ratios can be calculated. A typical result (at $1.5.10^{-2}$ torr and 190mA/cm^2) is shown in Table II. The results obtained compare well with test rig data using magnetic analysis of ions [3], [11] as is shown in Figure 3.

Optical spectra taken with the cryopumps filled with liquid nitrogen only, showed extra peaks with D_2 gas in the torus (Figure 2(b)). These peaks were due to back flow D_2 contamination of the source. The amount of D^+ at energy E_b was typically about 10% of the extracted H^+ current. This would be sufficient to cause a large increase in neutron production rate in a deuterium plasma, giving rise to large errors in plasma ion temperature measurements from neutron diagnostics. The use of liquid He filled cryopumps is sufficient to avoid such problems on DITE.

The current of hydrogen neutrals originating from impurities was typically about 4% of the total current from the main species ($j^o(E_b) + j^o(E_b/2) + j^o(E_b/3)$). To obtain this value a suitable estimate has been made for the H_α excitation cross section at low energies ($\sim$ 1.4keV), since no experimental data is available. The σ^o_ψ's are very slowly varying function of energy above 10keV and we have assumed that $\sigma^o_\psi(1.4\text{keV}) \simeq \sigma^o_\psi(10\text{keV})$.

To calculate the impurity ion current extracted from the source we use equation (10). The value of k' varies from $1(OH^+)$ to $5(CH_5^+)$. In most H_α profiles, structure was observed in the impurity peak (see Figure 2(c)) with the high point close to mass 19. We have taken the dominant impurities to be H_3O^+ and CH_5^+ and this leads typically to the extracted current ratios shown in Table II.

The number of neutral impurity atoms entering the torus can be estimated in the case of carbon where the relevant cross-sections have been measured [12,13]. The fraction of carbon atoms from methane break-up which is in the neutral state after traversing a gas target $n\ell$ (mols cm^{-2}) is given by:

$$f_o = 1 - \left[\frac{\sigma_{01}}{\sigma_{01} + \sigma_{10}} + \frac{\sigma_{10}}{\sigma_{01} + \sigma_{10}} \cdot \exp\left\{- n\ell(\sigma_{01} + \sigma_{10})\right\}\right] \quad \ldots (11)$$

where $\sigma_{01} \equiv$ cross section for ionisation $C + H_2 \rightarrow C^+ + \ldots\ldots$

$\sigma_{10} \equiv$ cross section for electron capture $C^+ + H_2 \rightarrow C + \ldots\ldots$

For the DITE Phase II system f_o(carbon) was ~ 0.57. Thus from Table II one can estimate the ratio of neutral carbon atoms to neutral hydrogen atoms entering the torus to be

$$j_c^o : \Sigma j_H^o(E) \simeq 0.009 \pm 0.005$$

4.2 NPA spectra

Figure 4 shows the NPA fast neutral energy spectrum obtained for both C line sources working at 24.5kV, 29.0A ($j^+ \simeq 200 mA/cm^2$) and a source filling pressure of $1.5.10^{-2}$ torr. The spectrum is corrected for detector efficiency and shows three main peaks at E_b/k, k = 1, 2 and 3 and a smaller peak at $k \sim 18$ or 19. The NPA does not have sufficient resolution to show any structure in the impurity peak.

Measurements were taken with a torus pressure of 10^{-5} torr and a toroidal field (B_ϕ) of 1.4T. For these conditions the time scale for loss of the circulating fast ions by charge exchange is $\sim 1/10$ of the time scale for loss to the torus walls by ∇B_ϕ and centrifugal drift. The count rate N(E) in an NPA peak can then be related to the initial flux ratio leaving the source by

$$\frac{j_k^+}{j_i^+} = \frac{N(E/k)}{N(E)} \frac{f^o(E)\sigma_{01}(E)}{k' f^o(E/k)\sigma_{01}(E/k)} \frac{\eta(E)}{\eta(E/k)} \quad \ldots (12)$$

where j_k^+ = ion current with mass k amu

$\sigma_{01}(E)$ = ionisation cross section at energy E

$\eta(E)$ = detector efficiency at energy E

k' = number of hydrogen nuclei yielded on breakup of original ion (for the main species $k' = k$)

Applying equation (12) to the energy spectrum one obtains the ratios for ions extracted from the source given in Table II in good agreement with the optical spectra results. Taking the impurity ion as H_3O^+ this gives the ratios shown in Table II, where it should be noted that in this case the cross sections used at the low energies (1-2keV) are measured values [14].

4.3 NIVUV measurements

Figure 5 shows the result of a spectral scan of emission from the C^{3+} doublet ($2s\ ^2S \rightarrow 2p\ ^2P$) for 150kA DITE discharges [$T_{eo} \sim 1$keV, $n_{eo} \sim 5.10^{19}\ m^{-3}$] before and during 1MW of neutral injection. A distinct feature was seen to the short wavelength side of the doublet when the injectors were on, indicating the presence of C^{3+} ions with energies of up to $\sim$ 20keV, in the direction of beam injection. This feature was completely absent when the injectors were off. This is convincing evidence for the presence of carbon in the neutral injection beam. A direct estimate of the carbon concentration could not be made from NIVIV measurements alone since the instrument was not capable of spatially scanning the plasma. Extreme ultra violet (EUV) measurements on DITE using a calibrated spatially scanning grazing incidence spectrograph indicate that the carbon content of the plasma (C^{5+}) in the absence of neutral injection was typically 1% of the electron concentration [15]. Using this result and the ratio of the shifted C^{3+} feature in Figure 5 to that of the line intensity with injection off, the carbon content of

the beam was estimated to be about 1.5%. This figure agrees well with the 0.9% neutral carbon content derived from the Doppler shifted H_α measurements.

A similar scan over the O^{6+} line at 162.3nm, Figure 6, shows no short wavelength feature with injection. However, with the injectors on, the line centre was shifted ~ 0.08nm to shorter wavelengths, corresponding to a toroidal plasma rotation velocity ~ 10^5 m/sec induced by the momentum of the injected beam. No such mass motion was observed on the C^{3+} line, probably because at the edge of the plasma where this line is produced viscosity damps out such effects.

The fact that no high energy (~ 20keV) O^{6+} ions were detected in the plasma does not necessarily mean the absence of oxygen in the neutral beam. Fast impurity neutrals injected with the beam are ionised and excited by electron impact, and slow down via proton collisions. Carbon atoms injected into the plasma are rapidly ionised to the C^{3+} state in a time << 1ms. In this state the slowing down time (proportional to $1/Z^2$) is ~ 5ms, which is considerably longer than both the timescale for excitation of the C^{3+} doublet (~ 0.1ms) and the timescale for ionisation to the C^{4+} state (~ 0.1ms). Hence the C^{3+} emission from injected impurities will be from fast ions. For oxygen, the ionisation time to O^{6+} is ~ 0.25ms. In this state the slowing down time is ~ 1.2ms, considerably shorter than the timescale for O^{6+} line emission (~ 4ms) and the ionisation time to O^{7+} (~ 10ms). Therefore the majority of the O^{6+} line emission from injected oxygen will come from ions with energies considerably less than the injection energy. Any such emission would tend to be masked by the Doppler shifted plasma impurity line. It was not possible to make measurements on lines from lower ionisation states of oxygen because of lack of signal.

Similar spectroscopic measurements have been made on the 2XIIB plasmas [16] of both Doppler broadening of O^{5+} and the spatial dependence of O^{1+} line emissions during injection. The oxygen content of the beams was estimated to be about 2%.

4.4 Investigation of source impurities

The origin of impurities in the beam was investigated by the following experiments:

(1) The source gas was contaminated with nitrogen, oxygen and water vapour to the level of 2-3% by allowing outgassing to occur in the source reservoirs over a period of one week. Residual gas analysis (RGA) of the source gas was used to measure contamination. This impurity level could be reduced by over two orders of magnitude by purging and flushing the reservoirs. RGA traces were taken after arcs had been struck in the plasma sources, and it was found that 'dirty' gas gave slightly higher methane and water vapour production. However, the enhancement factor was not significant and it was found to be impossible to distinguish between 'pure' or 'dirty' gas sources from the $E_b/17$-$E_b/19$ lines in the H_α spectrum. Methane is produced more copiously in the plasma source arc than water vapour (by a factor ~ 8) although the main H_α peak was at $E_b/19(H_3O^+)$.

(2) It seems likely that the observed impurities originate from the material of the plasma source itself. The source anode is a stainless steel box which was <u>not</u> vacuum baked before assembly and this could therefore be a source of water vapour. Carbon is present as a constituent of stainless steel. Previous measurements on a test rig have shown the decrease of the 'mass 19' peak with time [11], indicating discharge cleaning taking place. Since the magnetic cusp field at the

walls of a bucket source is designed to shield the anode from electrons and hence increase arc electrical efficiency [3], this discharge cleaning could not be effective over a very wide area. In an attempt to drive off water vapour in the stainless steel a new anode box was heated to 130°C for 24 hours yielding an outgassing rate in bench tests an order of magnitude below normal. However, when placed on the beam line this anode did not lead to any improvement in the impurity peak.

(3) There is some evidence that the amount of impurity present in the arc affects the ratio of the main species. This is indicated in Figure 7, where the relationship appears particularly strong for the $H^+ : H_2^+$ ratio, which increases with rising impurity content. The particle balance in a discharge source is very complex [17]. It can be shown however (see Appendix 1) that reactions of the type

$$H_3^+ + H_2O \rightarrow H_3O^+ + H_2$$

$$H_3^+ + CH_4 \rightarrow CH_5^+ + H_2$$

can compete with the normal ionic breakup reactions due to electron bombardment in the source and hence alter the species yield.

5. CONCLUSIONS

The experiments demonstrate that measurements in the DITE torus of injected hydrogen energy spectra using a scanning monochromator and neutral particle analyser yield species ratios in good agreement with each other and with standard test rig measurements.

The detection of hydrogen-bearing impurity ions in the beams is possible at contamination levels ~ 1%. The main impurity ions identified for the DITE Phase II system are H_3O^+ and CH_5^+ from water vapour and methane in the arc discharges of the plasma sources. The impurities

almost certainly arise by liberation from the source surface material (stainless steel). Impurity levels of between 1 and 6% of the ions accelerated by the source have been observed. It is probable that these levels will only be reduced by proper vacuum baking of all the source components.

Vacuum ultra-violet emission spectroscopy on DITE plasmas in the presence of neutral injection reveals the presence of fast ($\sim$ 20keV) C^{3+} ions arising from ionisation of carbon atoms from the injected beam. The calculated amounts are in overall agreement with the amount of CH_5^+ in the initial accelerated beams. Highly ionised oxygen (O^{6+}) ions do not exhibit such high velocities but show up the bulk rotation of the plasma due to momentum transfer of the injected beams. The lack of high energy O^{6+} is explicable in terms of relative slowing-down and excitation times and does not rule out the presence of oxygen atoms in the neutral beams. The lower ionisation states of oxygen are more likely to yield positive results but their intensity is insufficient in DITE for accurate measurements.

There is some evidence that the amount of impurity present affects the main species ratios ($H^+ : H_2^+ : H_3^+$) produced by the ion sources.

Backflow contamination of the hydrogen beam with deuterium when injecting into a deuterium plasma is removed by operating the beam line cryopumps at liquid helium temperatures. This isolates the sources from the torus gas flow.

ACKNOWLEDGEMENTS

We would like to thank A.F. Newman, J. Percival and Dr. R.D. Gill for their assistance and V.L. Dunkley for aid in the setting up of the apparatus. We are grateful to Dr. R.S. Hemsworth for enlightenment on the behaviour of the ion-molecule reactions and to Dr. A.R. Martin for bringing the data on carbon neutralisation and reionisation to our attention.

APPENDIX 1

ESTIMATION OF THE EFFECT OF IMPURITY MOLECULES ON THE NORMAL PRODUCTION OF HYDROGEN SPECIES IN A DISCHARGE SOURCE

The chain reactions leading to the production of hydrogen species in an ion source is very complex to analyse [17]. We here focus on one particular reaction, the breakup of H_3^+, to show how impurity molecules can affect the chain of events.

H_3^+ is formed in the ion source by ion-molecule collisions.

$$H_2^+ + H_2 \rightarrow H_3^+ + H \qquad \ldots (A1.1)$$

It can then be dissociated by collisions with the electrons in the source plasma. The principal reactions are breakup to neutral atoms, caused primarily by Maxwellian electrons:

$$\begin{aligned} H_3^+ + e &\rightarrow H + H + H \\ &\rightarrow H + H_2 \\ &\rightarrow H + H + H^+ + e \end{aligned} \qquad \ldots (A1.2)$$

and breakup to proton final states, arising mainly from the high energy (primary) electrons in the ion source:

$$\begin{aligned} H_3^+ + e &\rightarrow H + H + H^+ + e \\ &\rightarrow H_2 + H^+ \\ &\rightarrow H_2^+ + H + e \end{aligned} \qquad \ldots (A1.3)$$

The cross sections for reactions (A1.2) and (A1.3) have been measured [18,19,20] and allow estimates to be made of their rate of occurrence in the source. These estimates are given in Table III where the following parameters have been assumed for the ion source [21]:

temperature of Maxwellian electrons 2eV

density of Maxwellian electrons $\sim 10^{18}$ m^{-3}

energy of the primary electrons 90eV

density of the primary electrons $\sim 10^{17}$ m^{-3}

Impurity molecules of methane and water vapour can modify the H_3^+ breakup chain by the following ion-molecule reactions:

$$H_3^+ + CH_4 \rightarrow CH_5^+ + H_2 \quad \ldots (A1.4)$$

$$H_3^+ + H_2O \rightarrow H_3O^+ + H_2 \quad \ldots (A1.5)$$

Rate coefficients for reaction (A1.4) [22] and (A1.5) [23] have been measured and from the RGA traces of the arc gas we know that the partial pressures of methane and water vapour are 2.5% and 0.4% respectively. Thus at a source pressure of $1.5.10^{-2}$ torr we arrive at the rates of occurrence of reactions A1.4, A1.5 given in Table III. It can be seen that the ion-impurity molecule reactions are competitive with the electronic breakup reactions for the removal of H_3^+ and it is therefore plausible that this affects the main species' ratios produced by the source.

TABLE I

Values of $\tau_\psi A_{\alpha\psi}$ and K_ψ (see text) for the various beam components (E in keV)

State	$\tau_\psi A_{\alpha\psi}$	$K_\psi(E)$ E = 25	E = 12.5	E = 8.33	E = 1.4
3s	1.0	0.81	0.86	0.89	0.97
3p	0.118	1.0	1.0	1.0	1.0
3d	1.0	0.98	0.98	0.99	1.0

TABLE II

Typical results for the hydrogen energy spectrum and the source species ratios obtained at source pressure $1.5.10^{-2}$ torr and ion current density 190mA/cm^2

Measured quantity	Method	Result
Hydrogen spectrum entering torus (ignoring impurities)	H_α	$j_H^o(E_b) : j_H^o(E_b/2) : j_H^o(E_b/3)$ = 48.2 : 22.2 : 29.6%
Extracted species ratio leaving the source (ignoring impurities)	H_α	$j_1^+ : j_2^+ : j_3^+$ = 73.3 : 14.5 : 12.2%
Extracted species ratio leaving the source (ignoring impurities)	NPA*	$j_1^+ : j_2^+ : j_3^+$ = 69.0 ± 3.0 : 14.6 ± 0.8 : 16.4 ± 0.9%
Extracted species ratio leaving the source (including impurities)	H_α	$j_1^+ : j_2^+ : j_3^+ : j_{17}^+(CH_5^+) : j_{19}^+(H_3O^+)$ = 68.6 : 13.6 : 11.0 : 1.6 : 4.7%
Extracted species ratio leaving the source (including impurities)	NPA*	$j_1^+ : j_2^+ : j_3^+ : j_{19}^+(H_3O^+)$ = 65.9 ± 3.0 : 14.0 ± 0.8 : 15.7 ± 0.9 : 4.5 ± 0.5%

*Source current density = 200mA/cm^2.

TABLE III

Rates for electronic and impurity molecule reactions removing H_3^+ in the plasma source

Reaction	Rate Coefficient (m^3 sec^{-1} $particle^{-1}$)	Occurrence rate in the Phase II source (sec^{-1} ion^{-1})
$H_3^+ + e \rightarrow$ neutral atoms	5.1×10^{-14}	5.1×10^{4}
$H_3^+ + e \rightarrow$ protons	4.0×10^{-13}	4.0×10^{4}
$H_3^+ + CH_4 \rightarrow CH_5^+ + H_2$	1.6×10^{-15} (1)	2.1×10^{4} (2)
$H_3^+ + H_2O \rightarrow H_3O^+ + H_2$	4.3×10^{-15} (1)	0.9×10^{4} (2)

(1) Rate coefficient at $297^{o}K$
(2) At $1.5.10^{-2}$ torr source pressure

REFERENCES

[1] Gill, R.D. et al., contrib. paper IXth European Conf. on Controlled Fusion and Plasma Physics (proceedings), Oxford (1979), 150.

[2] Axon, K.B. et al., contrib. paper 8th International Conf. on Plasma Physics and Controlled Nuclear Fusion Research, Brussels 1980, to be published.

[3] Hemsworth, R.S., Stork, D. and Cole, H.C., contrib. paper AP3, ibid.

[4] Hemsworth, R.S. et al., contrib. paper Joint Varenna-Grenoble Int. Symp. on Heating in Toroidal Plasma (proceedings), Grenoble (1978).

[5] Model 1870, SPEX Industries Inc., Box 798, Metuchen NJ 08840, USA.

[6] Summers, D.D.R., Gill, R.D. and Stott, P.E., CLM-P514, UKAEA, Culham Laboratory (1978).

[7] Thomas, E.W., private communication 1979.

[8] Model E766, Rank Precision Instruments Ltd., London NW1.

[9] Hughes, R.H., Petefish, H.M. and Kisner, H., Phys. Rev. A5, (1972), 2103.

[10] Thomas, E.W., Excitation in Heavy Particle Collisions, Wiley Interscience, 1972.

[11] Stork, D. and Hemsworth R.S., contrib. paper 8th Symp. on Engineering Problems of Fusion Research (proceedings), IEEE, San Francisco, (1979), Vol II, 1024.

[12] Phaneuf, R.A., Meyer, F.W. and McKnight, R.H., Phys. Rev. A17, (1978), 534.

[13] Fogel, Ia.A., Ankudinov, V.A. and Pilipenko, D.V., Sov. Phys.-JETP, 8, (1959), 601.

[14] Barnett, C.F. et al., 'Atomic Data for Controlled Fusion Research'. ORNL-5206 (Vol I), Oak Ridge National Laboratory (1977).

[15] Hobby, M.G., private communication (1979).

[16] Drake, R.P. and Moos, H.W., Nucl. Fus. 19, (1979), 407.

[17] Martin, A.R. and Green, T.S., CLM-R159, UKAEA, Culham Laboratory (1976).

[18] Peart, B. and Dolder, K.T., J. Phys. B7, (1974), 1948.

[19] Peart, B. and Dolder, K.T., J. Phys. B7, (1974), 1567.

[20] Peart, B. and Dolder, K.T., J. Phys. B7, (1974), L143.

[21] Hemsworth, R.S., Stork, D., Burcham, J.N., Cole, H.C. and Coultas, J.C.S., to be submitted for publication in J. Phys. E.

[22] Burt, J., Dunn, J.L., McEwan, M.J., Sutton, M.M., Roche, A.E. and Schiff, H.I., J. Chem. Phys., 52, (1970), 6062.

[23] Betowski, D., Payzant, J.D., Mackay, G.I. and Bohme, D.K., Chem. Phys. Letts., 31, (2), (1975), 321.

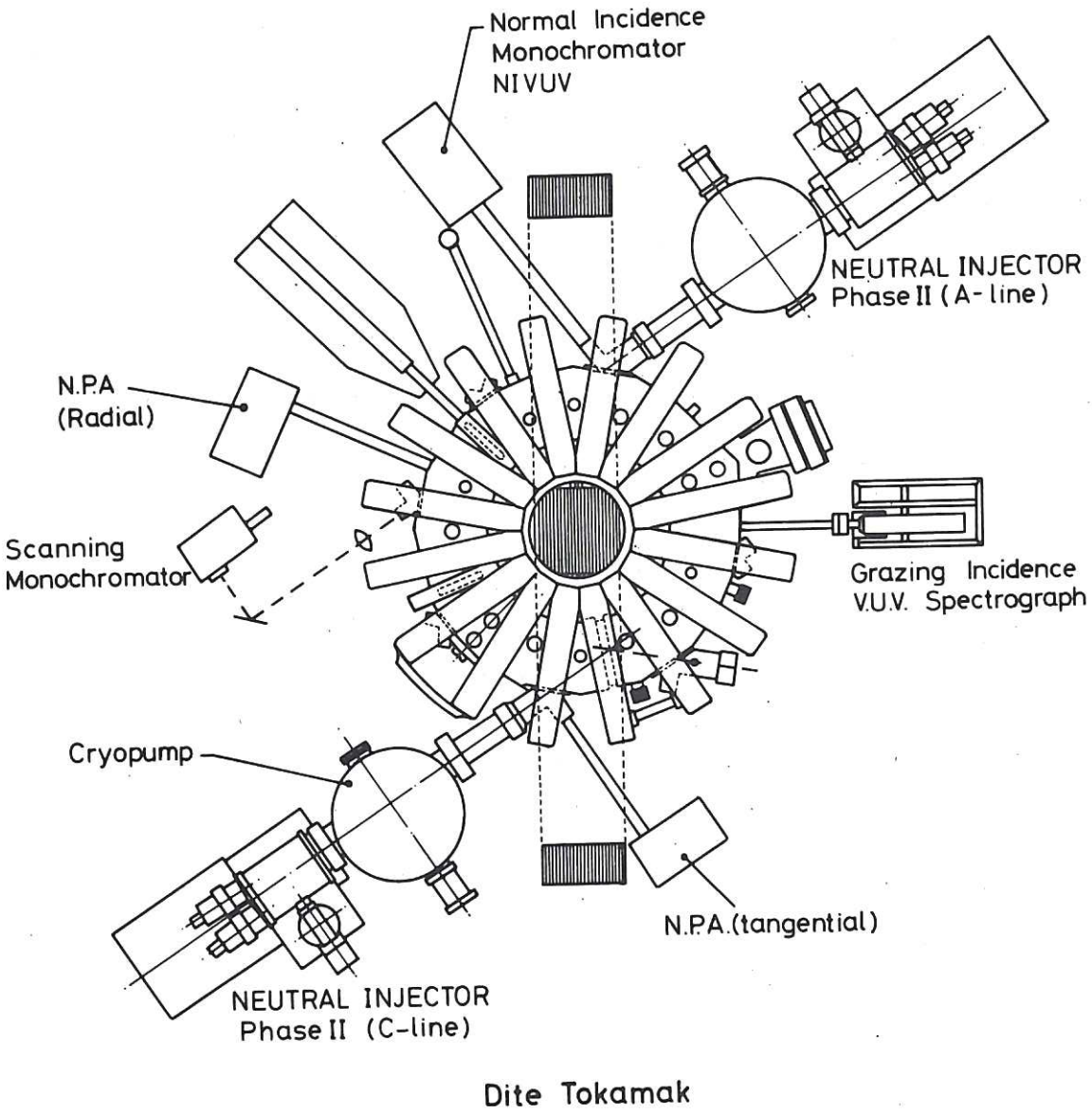

Fig.1 Plan view of DITE tokamak showing the neutral injection lines and the principal diagnostics.

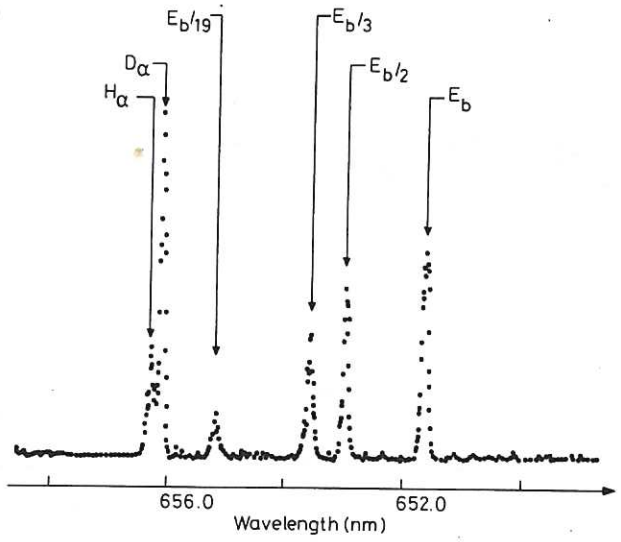

Fig.2(a) Digitised oscillogram of line emission around 656 nm for one A line source injecting into a D_2 filled torus, deflectors on, cryopumps at liquid He temperature.

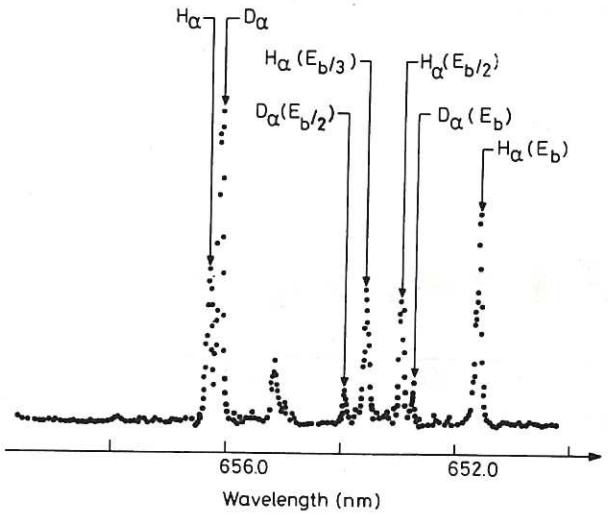

Fig.2(b) As for Fig.2(a), but cryopumps at liquid N_2 temperature.

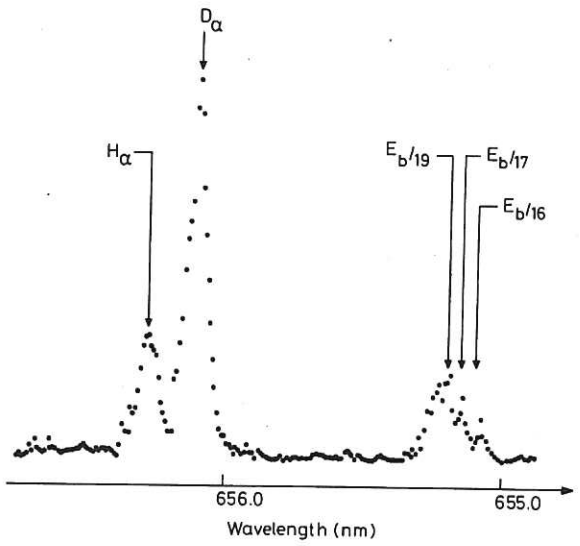

Fig.2(c) Digitised oscillogram of line emission around 656 nm for one A line source, torus filled with D_2, showing fine structure in the impurity peak.

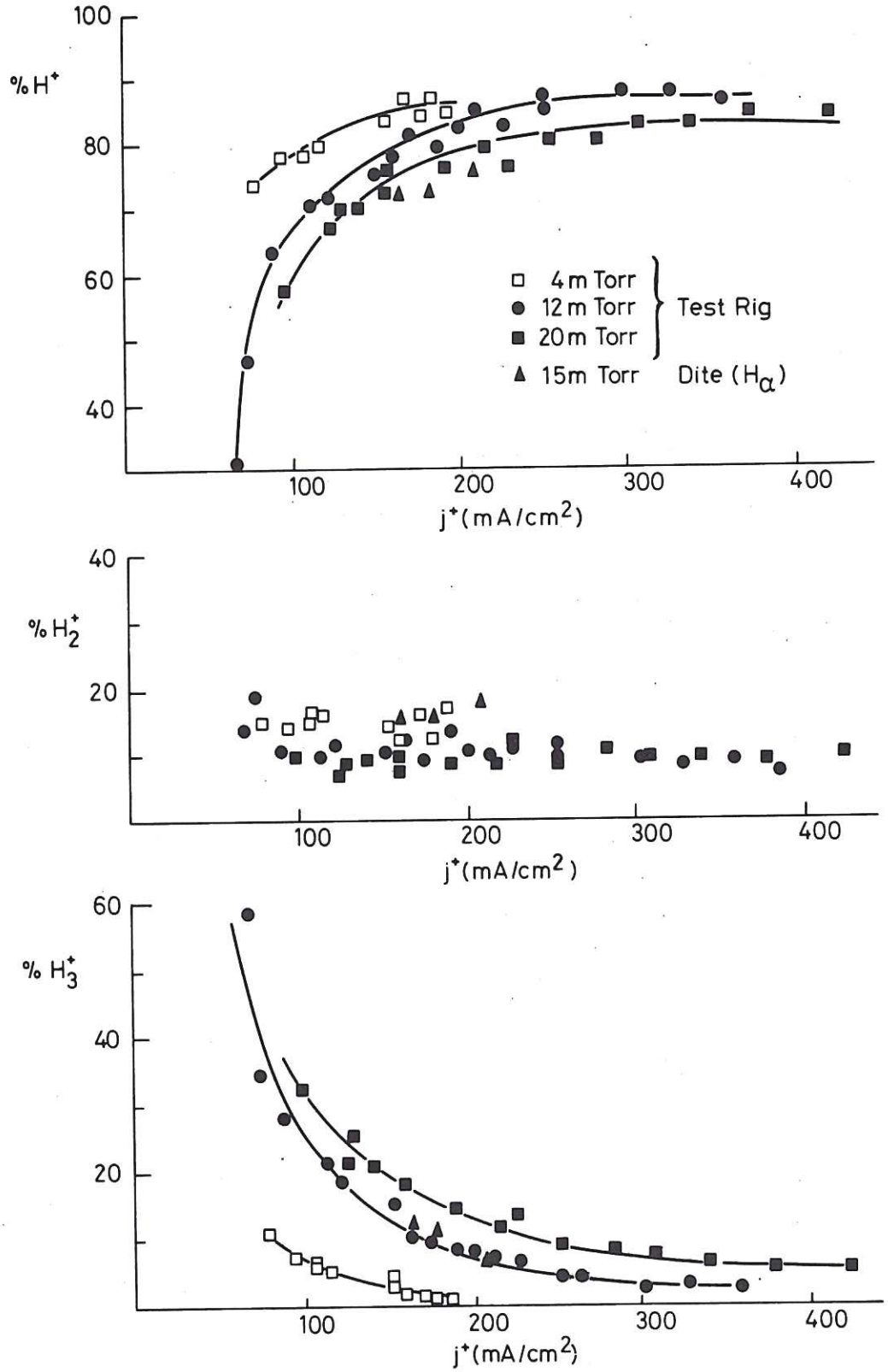

Fig.3 Comparison of species measurements made by Doppler spectroscopy on DITE, with test stand measurements using magnetic analysis of the extracted ions.

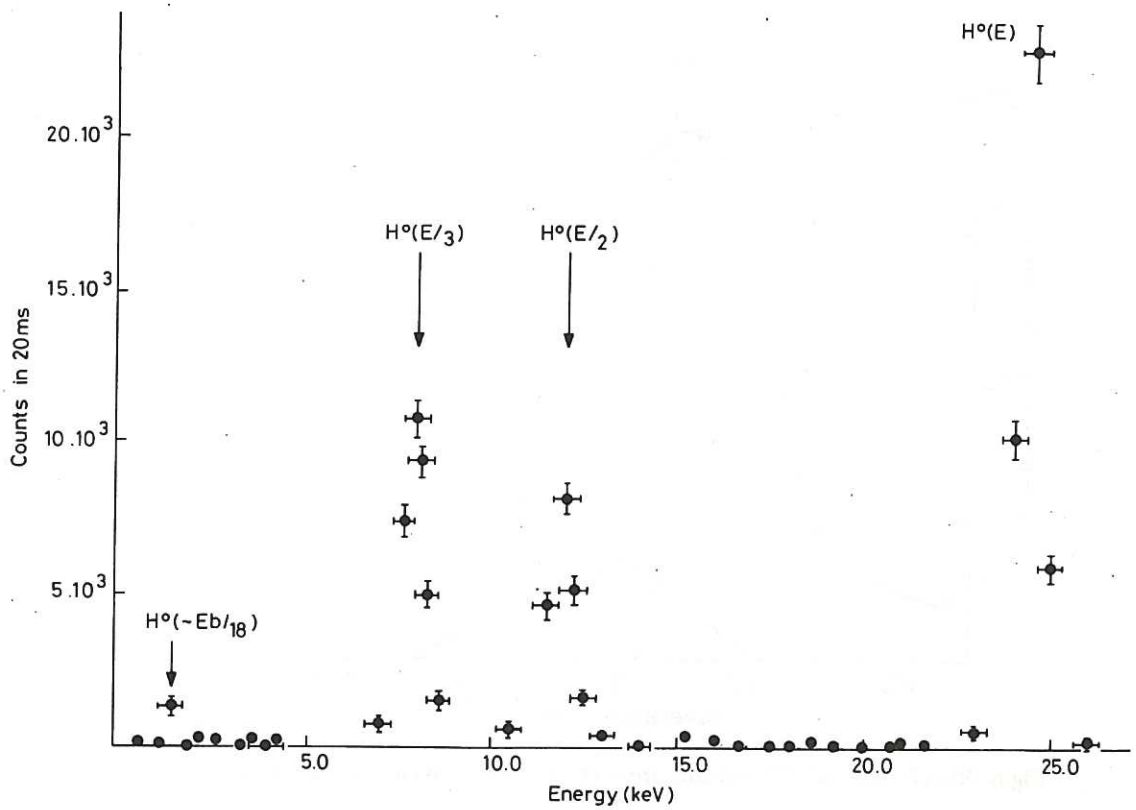

Fig.4 NPA fast neutral energy spectrum obtained with C line source injecting into a gas filled torus.

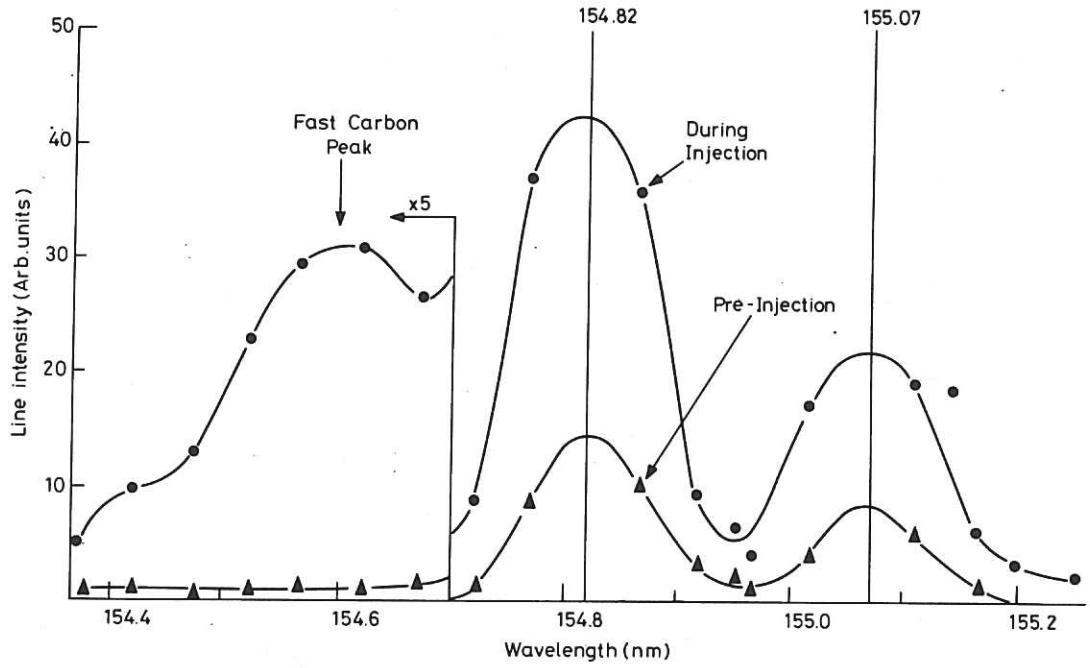

Fig.5 NIVUV scan of the C^{3+} doublet emission from 150kA DITE discharges, before and during injection.

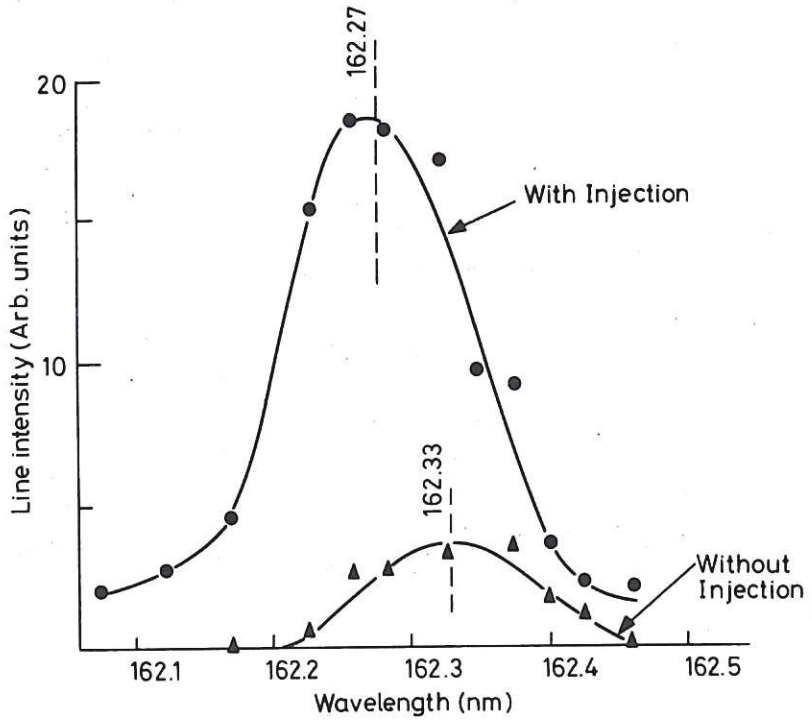

Fig.6 NIVUV scan of O^{6+} emission from DITE, before and during injection.

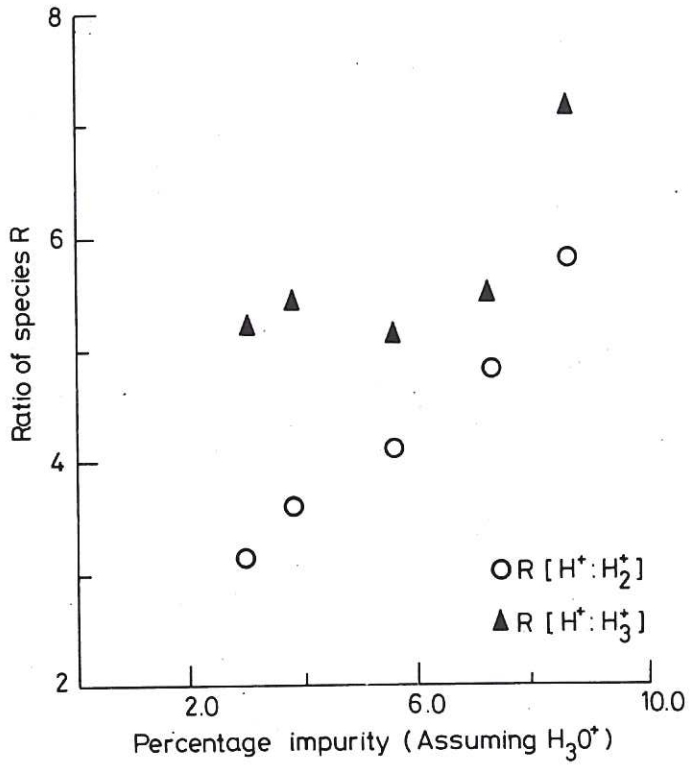

Fig.7 Variation of the ratio of the main hydrogenic species (H^+, H_2^+, H_3^+) with the amount of impurity (assumed to be H_3O^+) in the extracted beam.